J Mater Sci (2008) 43:4518–4526
DOI 10.1007/s10853-008-2647-5

Production and mechanical properties of metallic glass-reinforced Al-based metal matrix composites

S. Scudino · K. B. Surreddi · S. Sager · M. Sakaliyska · J. S. Kim · W. Löser · J. Eckert

Received: 9 October 2007 / Accepted: 11 April 2008 / Published online: 29 April 2008

Abstract Al-based metal matrix composites were synthesized through powder metallurgy methods by hot extrusion of elemental Al powder blended with different amounts of metallic glass reinforcements. The glass reinforcement was produced by controlled milling of melt-spun $Al_{85}Y_8Ni_5Co_2$ glassy ribbons. The composite powders were consolidated into highly dense bulk specimens at temperatures within the supercooled liquid region. The mechanical properties of pure Al are improved by the addition of the glass reinforcements. The maximum stress increases from 155 MPa for pure Al to 255 and 295 MPa for the samples with 30 and 50 vol.% of glassy phase, respectively. The composites display appreciable ductility with a strain at maximum stress ranging between 7% and 10%. The mechanical properties of the glass-reinforced composites can be modeled by using the *iso-stress* Reuss model, which allows the prediction of the mechanical properties of a composite from the volume-weighted averages of the components properties.

S. Scudino (✉) · K. B. Surreddi · M. Sakaliyska · J. Eckert
IFW Dresden, Institut für Komplexe Materialien,
Postfach 270116, D-01171 Dresden, Germany
e-mail: s.scudino@ifw-dresden.de

S. Sager
FG Physikalische Metallkunde, FB 11 Material- und Geowissenschaften, Technische Universität Darmstadt,
Petersenstraße 23, D-64287 Darmstadt, Germany

Present Address:
S. Sager
W.C. Heraeus GmbH, Heraeusstraße 12-14, 63450 Hanau, Germany

J. S. Kim
Research Center for Machine Parts and Materials Processing,
University of Ulsan, Namgu Mugeo 2-Dong, San 29,
Ulsan 680-749, Republic of Korea

W. Löser
IFW Dresden, Institut für Festkörperforschung, Postfach 270116,
D-01171 Dresden, Germany

J. Eckert
TU Dresden, Institut für Werkstoffwissenschaft, D-01062 Dresden, Germany

Introduction

Al-based metal matrix composites (MMCs) have been attracting considerable attention due to their remarkable mechanical properties, such as high elastic modulus and strength, and good fatigue and wear resistance, which renders them quite unique in comparison to conventional unreinforced materials [1–3]. Typical reinforcements in MMCs are ceramics, such as Al_2O_3 and SiC [1], and powder metallurgy (P/M) is one of the methods successfully used for the preparation of Al-based MMCs [1, 4, 5]. Besides ceramics, Al-based metallic glasses are particularly attractive as matrix reinforcements because of their extremely high strength at room temperature [6]. For example, high tensile strengths exceeding 1,200 MPa have been achieved for melt-spun Al–Ln–TM [7, 8] and Al–ETM–LTM [9] amorphous ribbons or amorphous wires prepared by melt-extraction [10]. Such strength levels are about twice as high as for conventional crystalline Al alloys [6].

Although Al-based amorphous alloys exhibit remarkable mechanical properties compared to conventional Al-based crystalline alloys, the maximum scale of the products is limited to a thickness less than 100 μm. This limitation of the Al-based amorphous alloys has prevented a wide extension of application fields even despite their excellent mechanical properties [6]. In fact, these alloys can only be

obtained by melt spinning in the shape of ribbons or by gas atomization in the form of powders [6]. No bulk amorphous single-phase alloys in Al-based systems have been obtained by any kind of solidification method up to date. This is due to the relatively low glass-forming ability of these systems [6].

Besides rapid quenching, solid-state techniques, such as mechanical alloying of elemental powder mixtures, have been employed to create glassy powders [11–16]. However, this approach presents problems in producing the same material by a processing route different than liquid quenching. For example, in contrast to rapid quenching, no complete amorphization is generally achieved by mechanical alloying for Al contents larger than 80 at.% [17], but the powders consist of an amorphous phase/fcc Al phase mixture, most likely coexisting with some intermetallic compounds.

Alternative to mechanical alloying, Al-based glassy powders can be produced by controlled milling of melt-spun glassy ribbons [18]. For example, melt-spun $Al_{85}Ni_9Nd_4Co_2$ glassy ribbons with a thickness of $\sim$25 μm and a width of $\sim$6 mm were ball milled at cryogenic temperatures [18]. By this, Al-based glassy powder can be produced in large quantities and the sticking problems, which normally occur during mechanical alloying of the pure elements with this composition (due to the high Al content of 85 at.%), can be avoided. Subsequent uni-axial hot pressing at temperatures within the supercooled liquid region leads to a density of about 94% in the bulk sample without crystallization [18].

In this work, glassy powders have been obtained by ball milling (BM) of melt-spun $Al_{85}Y_8Ni_5Co_2$ glassy ribbons. Due to the controlled milling conditions, the ball milled ribbons display a strikingly similar structure and crystallization behavior compared to the parent as-spun sample. The consolidation of the powders is a very complex procedure and the operational conditions, e.g. pressure, temperature, and holding time during the powder consolidation process, are difficult to be controlled precisely to obtain fully dense specimens without residual interfaces, which are a source of crack initiation and propagation between the powder particles. Accordingly, the crystallization behavior and the temperature dependence of the viscosity of the milled ribbon were studied to select the proper consolidation parameters. Glass-reinforced Al-based metal matrix composites were then consolidated through uni-axial hot pressing followed by hot extrusion and finally the mechanical properties of the bulk specimens were evaluated via room temperature compression tests.

Experimental

The starting materials for the melt spinning experiments were cylindrical rods with 10 mm diameter and 100 mm length. The rods of nominal composition $Al_{85}Y_8Ni_5Co_2$ were prepared from 99.9% pure elements by copper mold casting under argon atmosphere. Melt spinning experiments were carried out in a single-roller Bühler melt spinner at a speed of 30 m/s. The samples produced by this method were thin ribbons with a cross section of about 0.05×3 mm^2. Milling experiments on the glassy ribbons were performed using a Retsch PM400 planetary ball mill and hardened steel balls and vials. The ribbons were milled at cryogenic temperature for 5 h at a ball-to-powder mass ratio of 10:1 and at a rotational velocity of 150 rpm. The milling was carried out as a sequence of 15 min milling intervals interrupted by 15 min breaks to avoid a strong temperature rise. All sample handling was carried out in a glove box under purified argon atmosphere (less than 0.1 ppm O_2 and H_2O). Consolidation was done by uni-axial hot pressing (HP) and by hot extrusion under argon atmosphere at 520 K and 500 MPa. The density of the consolidated samples was evaluated by the Archimedes principle. The phases and the microstructure were characterized by X-ray diffraction (XRD) in transmission configuration using a STOE Stadi P diffractometer (Cu K_α radiation) and by scanning electron microscopy (SEM) using a JEOL JSM 6400 microscope. The thermal stability of the samples was investigated by differential scanning calorimetry (DSC) with a Perkin-Elmer Diamond calorimeter at 20 K/min heating rate under a continuous flow of purified argon. For all the DSC measurements, two successive runs were recorded with the second run serving as the base line. The calorimeter was calibrated for temperature and energy with high purity Indium and Zinc, giving an experimental error for the temperature and enthalpy of less than 1 K and 0.5 J/g, respectively. The viscosity of the samples as a function of the temperature was measured by parallel plate rheometry in a Perkin-Elmer TMA7 thermal mechanical analyzer (heating rate 10 K/min). Cylindrical specimens of 4 mm diameter and 8 mm length were prepared from the extruded samples whereas specimens with square section of 4×4 mm^2 and 8 mm length were prepared from the hot pressed samples. The specimens were tested with an INSTRON 8562 testing facility under quasistatic loading (strain rate of 8×10^{-4} s^{-1}) at room temperature. Both ends of the specimens were polished to make them parallel to each other prior to the compression test.

Results and discussion

Figure 1 shows the constant-rate heating DSC scan (20 K/min) of the as-spun $Al_{85}Y_8Ni_5Co_2$ ribbons. In the range of temperature considered the curve is characterized by a distinct glass transition (T_g), indicating the transformation from the solid-state glass into the supercooled liquid, followed by the supercooled liquid (SCL) region

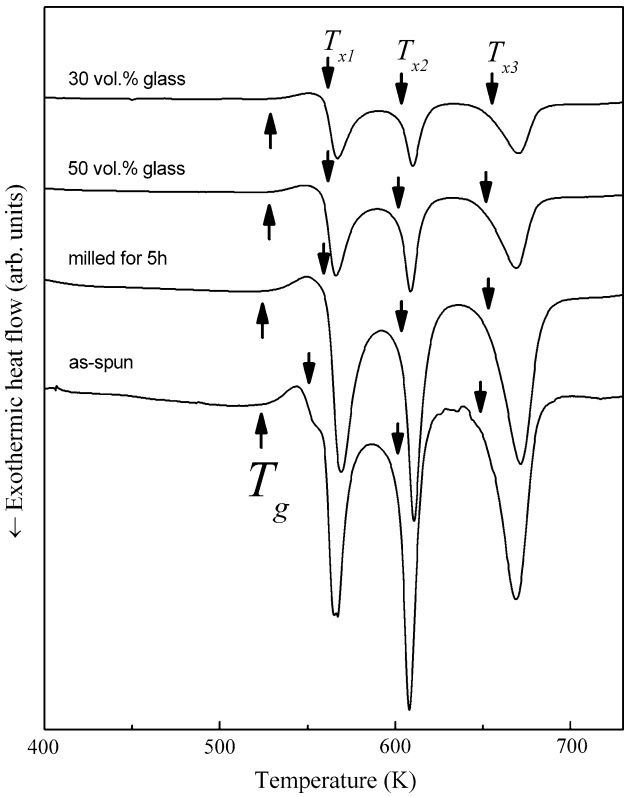

Fig. 1 DSC scans (20 K/min) for the as-spun $Al_{85}Y_8Ni_5Co_2$ ribbon, ribbon ball milled for 5 h and composite samples with 50 and 30 vol.% glass reinforcement

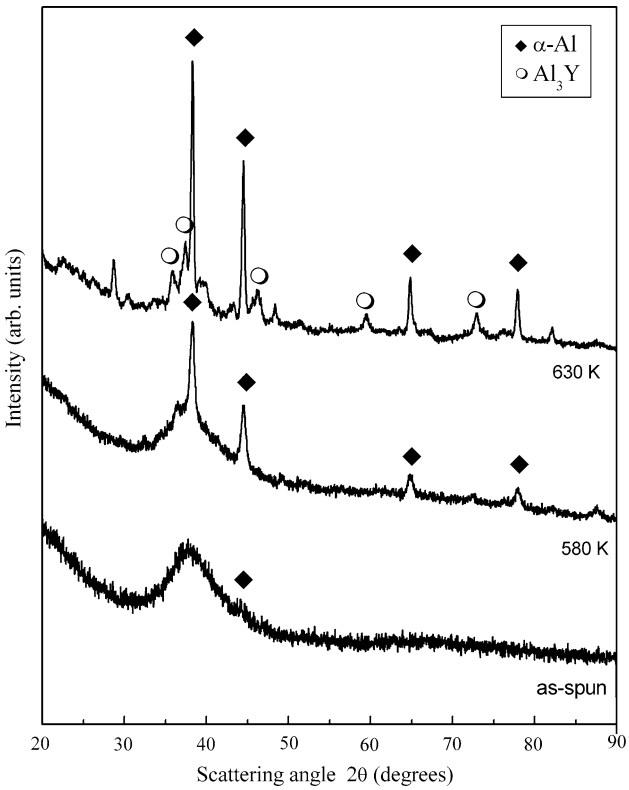

Fig. 2 XRD patterns (Cu-K_α radiation) for the as-spun $Al_{85}Y_8Ni_5Co_2$ glassy ribbon and ribbon heated at 20 K/min to completion of the first (580 K) and second (630 K) crystallization events

($\Delta T_x = T_{x1} - T_g$) before three exothermic heat flow events due to crystallization occur at higher temperature. The onsets of T_g and of the crystallization events (T_{x1}, T_{x2}, and T_{x3}) are 538, 560, 602, and 656 K, respectively. The SCL region, ΔT_x, is 22 K. The enthalpies of crystallization related to the exothermic DSC peaks are $\Delta H_1 = 32.1$ J/g, $\Delta H_2 = 36.4$ J/g, and $\Delta H_3 = 47.7$ J/g.

In order to study the structural evolution during heating, pieces of the as-spun ribbon were annealed in the DSC by continuous heating at 20 K/min up to different temperatures through the exothermic peaks followed by cooling to room temperature at 100 K/min. The phases formed were identified by X-ray diffraction and their patterns are shown in Fig. 2. The as-spun ribbons show the typical broad maxima characteristic for amorphous material together with a broad diffraction peak at about $2\theta = 44°$, most likely due to the formation of a small amount of fcc Al. When the sample is heated to 580 K, i.e. above the first crystallization peak, the XRD pattern displays the formation of fcc Al (space group *Fm*3*m*) [19]. Additionally, an overlapping broad diffraction maximum due to the residual amorphous phase can be observed. Heating to the completion of the second exothermic DSC peak (630 K) leads to the formation of the Al_3Y phase (space group *R*-3*m*) [19]. At the same time, the diffraction peaks belonging to the fcc Al phase become sharper, indicating grain growth.

Glassy powders with composition $Al_{85}Y_8Ni_5Co_2$ were produced by ball milling of melt-spun ribbons. The pulverization of the ribbons was achieved by using proper milling conditions, i.e. interval-milling at low intensity, corresponding to a rather low kinetic energy, and performed at cryogenic temperature to retain their glassy structure and to avoid sticking of the material to the milling tools due to the high ductility of the ribbons [18].

The effects of milling on the thermal stability and the microstructure of the melt-spun $Al_{85}Y_8Ni_5Co_2$ ribbon are shown in Figs. 1 and 3, respectively. Milling for 5 h does not change the multi-step crystallization behavior characterizing the as-spun ribbon. The values of T_g, T_{x1}, T_{x2}, and T_{x3} for the milled ribbon are 543, 562, 604, and 653 K and are, therefore, only slightly changed with respect to the as-spun ribbon. The enthalpies of crystallization were found to be $\Delta H_1 = 30.4$ J/g, $\Delta H_2 = 27.2$ J/g, and $\Delta H_3 = 41.9$ J/g. This indicates that the first crystallization event is marginally affected whereas the subsequent events are much more influenced by the milling treatment. The mechanical deformation does not induce crystallization of the glass, as illustrated by the XRD pattern of the ribbon milled for 5 h (Fig. 3), which, besides the broad diffraction peak already observed in the as-spun ribbon, does

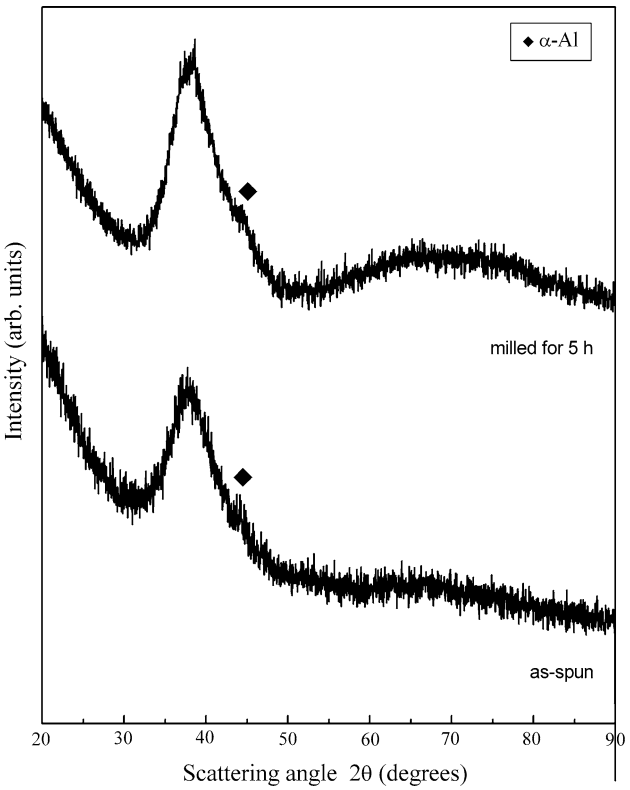

Fig. 3 XRD patterns (Cu-K_α radiation) for the as-spun $Al_{85}Y_8Ni_5Co_2$ glassy ribbon and ribbon ball milled for 5 h

not show additional crystalline precipitates. These results indicate that $Al_{85}Y_8Ni_5Co_2$ glassy powders displaying strikingly similar structure and crystallization behavior compared to the parent as-spun sample can be produced by pulverization of glassy precursors by carefully controlling the milling conditions.

In order to produce glass-reinforced MMCs, elemental Al powder was blended with different amounts of $Al_{85}Y_8Ni_5Co_2$ milled ribbons and the resulting powders were milled for 10 min to obtain a homogeneous dispersion of the glass reinforcement. The DSC scans of the MMCs with 50 and 30 vol.% of glassy phase are shown in Fig. 1. The presence of pure Al does not change the overall crystallization behavior. In fact, the values of T_g, T_{x1}, T_{x2}, and T_{x3} were found to be 269, 286, 329, and 377 K for the sample with 50 vol.% of glass and 272, 287, 330, and 378 K for the sample reinforced by 30 vol.% of glassy phase. These values are remarkably similar to the as-spun as well as to the milled ribbons. The enthalpies of crystallization are $\Delta H_1 = 13.6$ J/g, $\Delta H_2 = 11.5$ J/g, and $\Delta H_3 = 18.1$ J/g for the sample with 50 vol.% glass and $\Delta H_1 = 9.9$ J/g, $\Delta H_2 = 8.1$ J/g, and $\Delta H_3 = 12.7$ J/g for the sample containing 30 vol.% of glassy phase, which, after normalization by the vol.% of glass reinforcements, gives similar values with respect to the single-phase milled ribbons.

The thermal stability investigations of the milled powders reveal a distinct glass transition followed by a supercooled liquid region. In this region the powders exhibit a deformation regime characterized by a viscous flow behavior [13] that may allow the production of bulk samples by hot consolidation at temperatures within the range of the supercooled liquid region [13]. A better insight into the flow behavior within the SCL can be derived from viscosity measurements using parallel plate rheometry [20]. Accordingly, the proper consolidation temperature was selected by studying the influence of temperature on the viscosity of the ribbon milled for 5 h (Fig. 4). The viscosity η can be derived from the change of the height of the sample versus time as [20, 21]

$$\eta = \left(\frac{2Fh^3}{3\pi a^4(\mathrm{d}y/\mathrm{d}t)}\right), \quad (1)$$

where F is the applied load, a is the radius of the plates, and h is the height of the sample. This allows viscosity measurements in the range from 10^5 to 10^9 Pa s [20, 21]. The apparent viscosity decreases with increasing temperature from about 1.4×10^{10} Pa s at about 400 K to 2.1×10^9 Pa s at 520 K, most likely due to structural relaxation. As the glass transition temperature is reached (above 520 K) and the glassy solid transforms into the SCL, the curve displays a stronger viscosity drop. At about

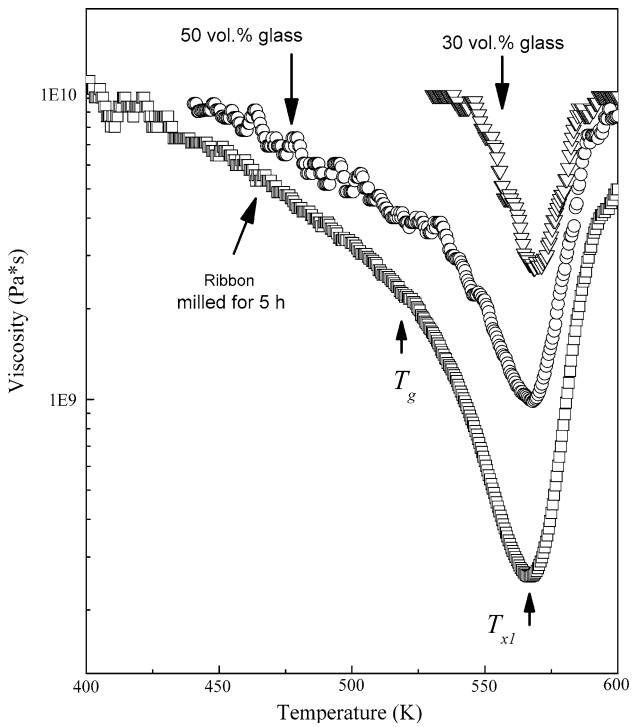

Fig. 4 Temperature dependence (heating rate 10 K/min) of the viscosity of the supercooled liquid for the single-phase $Al_{85}Y_8Ni_5Co_2$ glassy ribbon milled for 5 h and for the composite samples with 50 and 30 vol.% glass reinforcement

565 K crystallization sets in and the viscosity abruptly increases with increasing temperature, indicating the loss of liquid-like behavior. The values of T_g and T_{x1} evaluated from the viscosity measurements are in good agreement with the data determined from the constant-rate heating DSC scans given the different heating rate used for the experiments (10 K/min for η and 20 K/min for DSC). Similar results were observed for the MMCs with different volume fractions of $Al_{85}Y_8Ni_5Co_2$ glass (Fig. 4).

The MMCs with different amounts of glass reinforcements were consolidated by hot pressing followed by hot extrusion. Consolidation was performed at 520 K, to take advantage of the viscosity drop in the supercooled liquid regime, using a pressure of 500 MPa. By using these consolidation parameters, extrusion was performed in 10 min, a sufficiently short consolidation time to avoid crystallization of Al-based glassy powders [18]. For comparison purposes, a bulk specimen was produced by extrusion of pure Al powders using the same consolidation parameters as used for the MMCs. In addition, a single-phase $Al_{85}Y_8Ni_5Co_2$ glassy sample was consolidated by hot pressing. No extrusion of the hot pressed single-phase glass was possible in the present consolidation conditions.

Figure 5 shows the relative density of the consolidated samples as a function of the volume fraction of glass reinforcement. The relative density of the specimens with respect to the density of the starting materials used for the melt spinning experiments (i.e., the cylindrical rods of crystalline intermetallic compounds) decreases from 99.2% for the sample with 30 vol.% of glass reinforcement to 97.4% for the specimen with 50 vol.% of glassy phase and, finally, to 96.7% for the single-phase glass (100 vol.%). A similar behavior was reported for Al-based MMCs reinforced with SiC particles [22, 23] and was ascribed to clustering of the reinforcing particles [23].

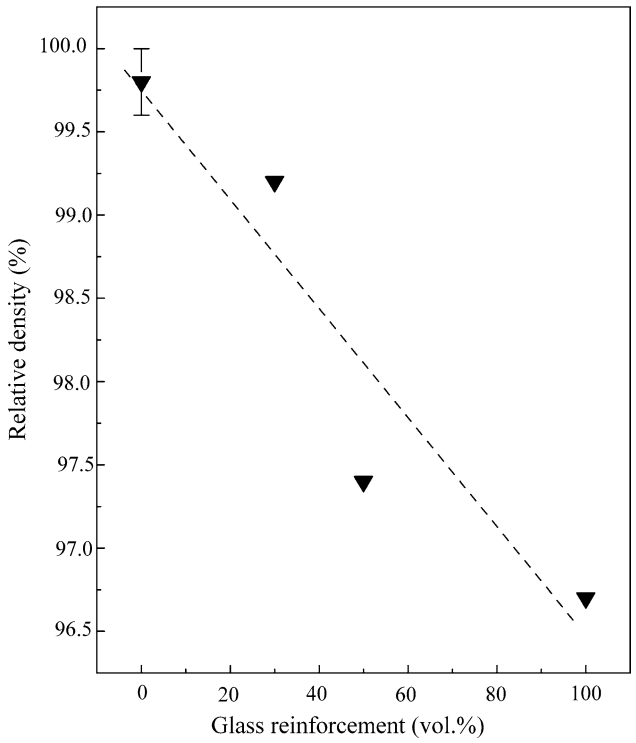

Fig. 5 Relative density of the consolidated samples as a function of the volume fraction of glass reinforcement

Figure 6a and b shows SEM images of the composites with 30 and 50 vol.% glass reinforcement, respectively. The images display a homogeneous distribution of flake-shaped particles (the glassy phase) dispersed in the fcc Al matrix. No porosity is visible, further corroborating the high density of the samples. On the other hand, the SEM image of the single-phase $Al_{85}Y_8Ni_5Co_2$ glassy specimen produced by hot pressing of the milled ribbons (Fig. 6c) displays a large number of pores. This indicates that incomplete bonding between the particles has occurred during consolidation, leading to a rather poor densification of the material.

As a typical example of the structure of the consolidated composites, Fig. 7 shows the XRD pattern of the MMC with 50 vol.% of $Al_{85}Y_8Ni_5Co_2$ milled ribbon. The pattern is characterized by few narrow diffraction peaks belonging to the fcc-Al phase together with the broad maximum belonging to the glassy phase at about $2\theta = 39°$. This indicates that no crystallization of the glass occurred during consolidation of the composites.

Typical room temperature uni-axial compression-true stress–true strain curves of the tests under quasistatic loading for the composite materials are shown in Fig. 8 together with the curves for pure Al and the single-phase glass. The observed fracture strains exceed 40% for all the composite materials; however, due to the strong softening characterizing the composite specimens after reaching the maximum stress, the compression tests shown in Fig. 8 were stopped after reaching the maximum strength and before fracture occurrence. Pure Al exhibits an elastic regime of 0.2% before yielding, which occurs at about 75 MPa. After yielding the stress increases with increasing strain, and the sample exhibits work-hardening up to the maximum stress of 155 MPa, reaching a strain at maximum stress of about 25%. The mechanical properties of pure Al are remarkably increased by the addition of the glass reinforcement. The specimen containing 30 vol.% glass displays an elastic regime of 0.3% and a yield strength of 120 MPa. The maximum stress is raised to 255 MPa while retaining a strain at maximum stress of about 10%. When the amount of glassy phase is further increased to 50 vol.% the elastic range is still 0.3% while the yield and maximum stress further increase to 130 and 295 MPa, respectively, and the strain at maximum

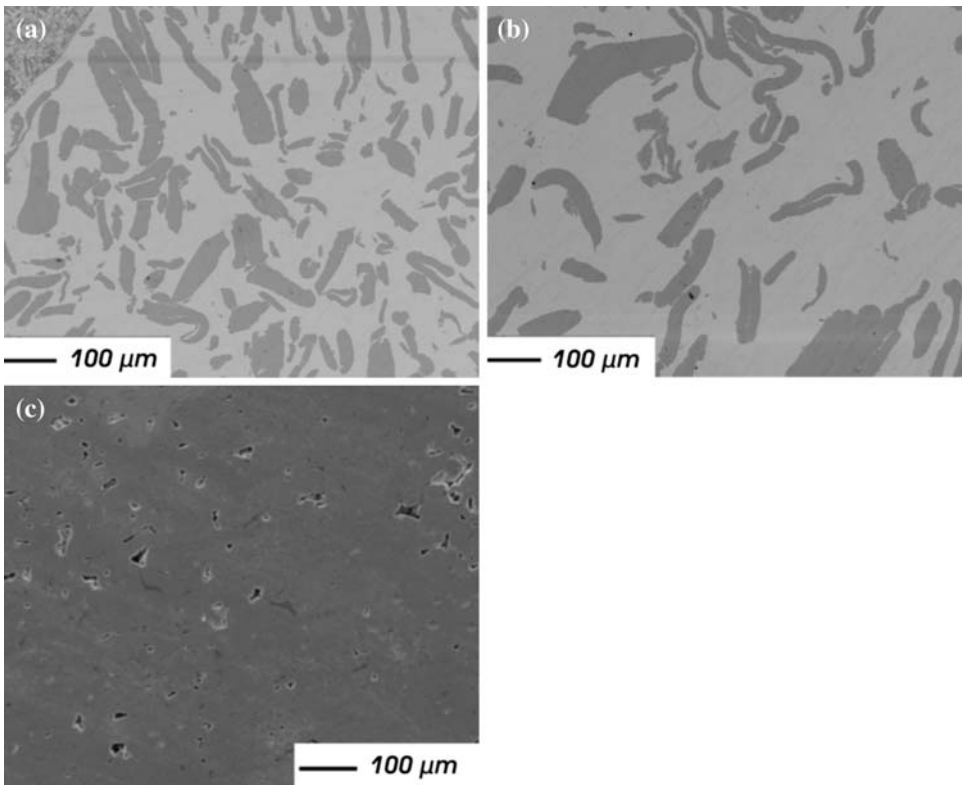

Fig. 6 SEM micrographs for the hot extruded composites with (**a**) 30 vol.% and (**b**) 50 vol.% glass reinforcement, and (**c**) hot pressed single-phase $Al_{85}Y_8Ni_5Co_2$ glassy powder

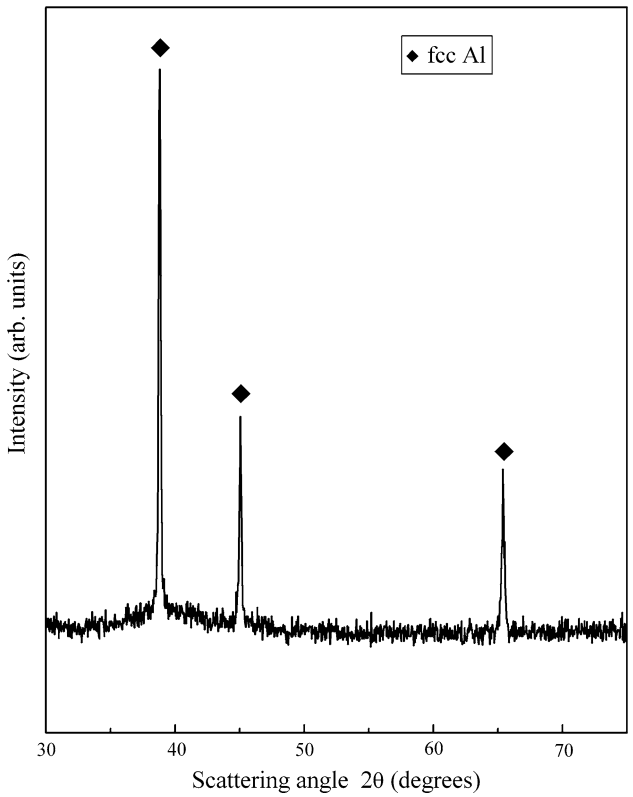

Fig. 7 XRD patterns (Cu-K_α radiation) for the hot pressed and hot extruded composite with 50 vol.% of $Al_{85}Y_8Ni_5Co_2$ glass reinforcement

stress is found to be about 7%. Finally, the single-phase $Al_{85}Y_8Ni_5Co_2$ glass produced by hot pressing only exhibits an elastic regime of 1.45% and a maximum stress of about 400 MPa, which is remarkably lower than that observed for melt-spun ribbons with the same composition (1,250 MPa) [24]. This is most likely due to the residual porosity and to the imperfect particle bonding characterizing the sample, which may lead to the early failure of the material.

The prediction of the overall mechanical properties of a composite from the properties of the single constituents is an important prerequisite for the material design and application. Among the different methods for estimating the mechanical properties of a composite, the rule of mixtures (ROM) is the simplest and the most intuitive [25, 26]. The ROM considers the properties of the composite as volume-weighted averages of the components properties and assumes that the components are non-interacting during deformation [27]. This approach has been extensively used to model the mechanical properties of fiber-reinforced matrix composites [27, 28]. Two ROM methods have been widely employed to predict the mechanical properties of composites [25, 28]: (i) the Voigt model, based on the equal strain assumption and (ii) the Reuss model, based on the equal stress assumption. Although these models have been derived for the elastic properties of composites, they have been also used for the overall plastic regime [25, 24, 28–30].

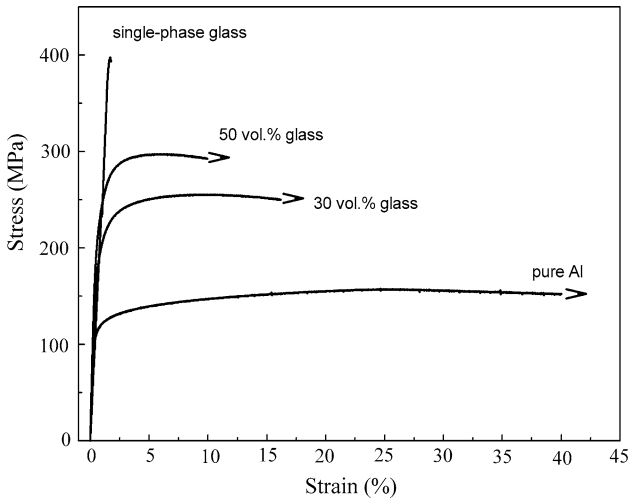

Fig. 8 Room temperature compression stress–strain curves for the hot pressed and hot extruded pure Al, hot pressed and hot extruded composite with 30 vol.% of $Al_{85}Y_8Ni_5Co_2$ glass reinforcement, hot pressed and hot extruded composite with 50 vol.% glass reinforcement and hot pressed single-phase $Al_{85}Y_8Ni_5Co_2$ glassy powder

The Voigt or *iso-strain* model assumes that the two components, matrix and reinforcement, experience the same strain during deformation [27]. For the stress of the glass-Al matrix composite [31], this can be written as:

$$\sigma_c = V_{gl}\sigma_{gl} + V_{Al}\sigma_{Al} \quad (2)$$

where V is the volume fraction, σ is the strength, and the subscripts c, gl, and Al indicate the composite, the glass reinforcement, and the Al matrix, respectively. It is often observed that the strength of a composite is lower than predicted by the Voigt model [32]. This is generally attributed to (i) inadequate bonding, (ii) porosity, and (iii) inherent material defects, e.g. cracks [32]. Therefore, the *iso-strain* treatment represents the upper bound.

The lower bound is given by the Reuss or *iso-stress* model, which assumes that the composite exhibits equal stress in the two components [27]. For the stress, this can be written as:

$$\sigma_c = \left(\frac{V_{gl}}{\sigma_{gl}} + \frac{V_{Al}}{\sigma_{Al}}\right)^{-1} \quad (3)$$

The effect of the porosity on the mechanical properties of a composite can be taken into account by considering the volume of the composite material to be made up of three different volumetric components, i.e. reinforcement, matrix, and porosity [33]:

$$V_c = V_{gl} + V_{Al} + V_p, \quad (4)$$

where the subscript p denotes the porosity.

The values of the maximum stress and the strain at maximum stress as a function of the amount of the $Al_{85}Y_8Ni_5Co_2$ glass reinforcement are shown in Fig. 9a

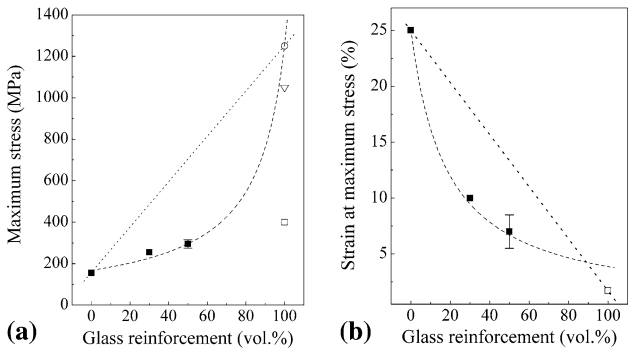

Fig. 9 (**a**) Maximum stress and (**b**) strain at maximum stress (evaluated from Fig. 8) as a function of volume percent of glass reinforcement for the samples: (■) hot extruded, (□) hot pressed, (○) single-phase $Al_{85}Y_8Ni_5Co_2$ melt-spun glassy ribbon from Ref. [24], and (▽) calculated from Eq. 3 (see text)

and b together with the values of the glassy ribbon [24] and of the single-phase glass consolidated by hot pressing (present work). The strength of the samples strongly deviates from the Voigt model (dotted line) and, instead, can be fitted well by using the Reuss model [corrected for porosity by Eq. 4] (dashed line). This behavior indicates that the compressive strength obeys the *iso-stress* model. The significant difference in strength observed between the single-phase $Al_{85}Y_8Ni_5Co_2$ glass consolidated by hot pressing (400 MPa) and the melt-spun glassy ribbon with the same composition (1,250 MPa) [24] cannot be exclusively ascribed to the effect of porosity. In fact, the maximum stress of a melt-spun ribbon with the density of the HP glass calculated by Eq. 3 should exceed 1,000 MPa [open triangle in Fig. 9a]. Most likely, the considerably low strength of the HP sample is due to inadequate bonding between the particles.

Figure 9b shows the strain at maximum stress for the different composite materials. No values for the strain are available for a fully dense glassy specimen [such as for the melt-spun glassy ribbon in Fig. 9a]. Therefore, the strain value of the low-density single-phase $Al_{85}Y_8Ni_5Co_2$ glass consolidated by HP was used in the data fitting. Similar to the maximum stress values in Fig. 9a, the corresponding strain at maximum stress can be well fitted using the *iso-stress* Reuss model. Although lower than predicted by the Reuss model, the strain of the HP specimen follows the *iso-stress* treatment within the experimental error. This indicates that the poor particle bonding is less significant in affecting the strain of the single-phase glass.

The validity of the Reuss model for the description of the composites studied in the present work is justified by the following considerations. The milled ribbons used as reinforcements are in the form of flake-shaped particles. Therefore, they can be treated as short fibers as a first approximation. Although not aligned along the same

direction, they tend to lie on the same plane (see Fig. 6a and b), which is normal to the applied stress during the compression test. Therefore, such composites can be considered as a random fiber array in a matrix deformed perpendicularly to the fiber direction, the latter being a requirement for the application of the *iso-stress* model [27]. In addition, it has been reported that the Voigt model fits the data well for a high volume fraction of reinforcement [26]. In this case, the deformation affects the reinforcements as a consequence of the smaller distance between the particles/fibers [26]. On the other hand, the Reuss model works well for small volume fractions and longer distances between the reinforcements, where the deformation mainly occurs in the soft matrix [26]. In the current work, the amount of reinforcements is relatively low (≤50 vol.%) and the distance between the particles is large (>50 μm). Therefore, most likely the plastic deformation occurs mainly in the matrix and the mechanical properties obey the *iso-stress* model.

Conclusions

Glass-reinforced Al-based MMCs with high strength combined with considerable ductility have been produced by powder metallurgy methods. $Al_{85}Y_8Ni_5Co_2$ glassy powders were produced by pulverization of the melt-spun glassy ribbons. To retain their glassy structure and to avoid sticking of the material to the milling tools due to the high ductility of the ribbons, proper milling conditions were used (i.e. interval-milling at low intensity, corresponding to a rather low kinetic energy, performed at cryogenic temperature). The MMCs with different amounts of glass reinforcements were consolidated into bulk specimens by hot pressing followed by hot extrusion at temperatures within the supercooled liquid region. The addition of the glass reinforcement remarkably improves the mechanical properties of fcc Al. The maximum stress increases from 155 MPa for pure Al to 255 and 295 MPa for the samples with 30 and 50 vol.% of glassy phase, respectively, while retaining appreciable ductility. The single-phase $Al_{85}Y_8Ni_5Co_2$ glass was consolidated by hot pressing alone. No extrusion of the single-phase glass was possible at temperatures below the crystallization temperature. Room temperature compression tests of the single-phase glass reveal low strength and no ductility due to the residual porosity of the consolidated specimen. The mechanical properties of the glass-reinforced composites can be modeled by using the *iso-stress* Reuss model, which allows the prediction of the mechanical properties of a composite from the volume-weighted averages of the components' properties.

Acknowledgements The authors would like to thank B. Bartusch, M. Frey, H.-J. Klauß, and H. Schulze for technical assistance, and M. Stoica, S. Venkataraman, and P. Yu for stimulating discussions. This work was supported by the German Science Foundation under grant Ec 111/16–2.

References

1. Kainer KU (2006) In: Metal matrix composites. Custom-made materials for automotive and aerospace engineering. Wiley-VCH Verlag GmbH & Co, Weinheim
2. Embury JD, Lloyd DJ, Ramachandran TR (1989) Strengthening mechanisms in aluminum alloys. In: Vasudevan AK, Doherty RD (eds) Aluminum alloys—contemporary research and applications, vol 31, Ch 22. Academic Press, Inc., p 579
3. Murakami Y (1996) Aluminum-based alloys. In: Cahn RW, Haasen P, Kramer EJ (eds) Materials science and technology, vol 8, Ch 5. VCH, p 213
4. Hildeman GJ, Koczak MJ (1989) Powder-metallurgy aluminum alloys. In: Vasudevan AK, Doherty RD (eds) Aluminum alloys—contemporary research and applications, vol 31, Ch 11. Academic Press, Inc., p 323
5. Yu P, Kim KB, Das J, Baier F, Xu W, Eckert J (2006) Scripta Mater 54:1445. doi:10.1016/j.scriptamat.2006.01.001
6. Inoue A (1998) Prog Mater Sci 43:365. doi:10.1016/S0079-6425(98)00005-X
7. He Y, Poon SJ, Shiflet GJ (1988) Science 241:1640. doi:10.1126/science.241.4873.1640
8. Inoue A, Ohtera K, Tsai AP, Masumoto T (1988) Jpn J Appl Phys 27:L280. doi:10.1143/JJAP.27.L280
9. Tsai AP, Inoue A, Masumoto T (1988) Metall Trans A 19:1369 doi:10.1007/BF02662599
10. Inoue A, Amiya K, Yoshii I, Kimura HM, Masumoto T (1994) Mater Trans JIM 35:485
11. Afonso CRM, Oliveira MFd, Bolfarini C, Botta Filho WJ, Kiminami CS (2003) Mater Sci Forum 416–418:388
12. Fjeldly A, Roven HJ (1996) Acta Mater 44:3497. doi:10.1016/1359-6454(96)00015-8
13. Eckert J (1997) Mater Sci Eng A 226:364. doi:10.1016/S0921-5093(96)10646-8
14. Eckert J, Schultz L, Urban K (1988) J Less-Comm Metals 145:283
15. Eckert J, Schultz L, Hellstern E, Urban K (1988) J Appl Phys 64:3224. doi:10.1063/1.341540
16. Börner I, Eckert J (2001) Scripta Mater 45:237. doi:10.1016/S1359-6462(01)01026-0
17. Seidel M, Eckert J, Bauer HD, Schultz L (1995) In: Otooni MA, Armstrong RW, Grant NJ, Ishizaki K (eds) Grain size and mechanical properties—fundamentals and applications. Mater. Res. Soc. Symp. Proc., Materials Research Society, Warrendale, PA, p 239
18. Calin M, Grahl H, Adam M, Eckert J, Schultz L (2004) J Mater Sci 39:5295. doi:10.1023/B:JMSC.0000039232.67075.ed
19. Villars P, Calvert LD (1985) In: Villars P, Calvert LD (eds) Pearson's handbook of crystallographic data for intermetallic phases. Metals Park (OH), American Society for Metals
20. Busch R, Bakke E, Johnson WL (1998) Acta Mater 46:4725. doi:10.1016/S1359-6454(98)00122-0
21. Deledda S, Eckert J, Schultz L (2004) Mater Sci Eng A 375–377:804. doi:10.1016/j.msea.2003.10.027
22. Chung WS, Chang SY, Lin SJ (1999) J Mater Res 14:803. doi:10.1557/JMR.1999.0106
23. Slipenyuk A, Kuprin V, Milman Y, Goncharuk V, Eckert J (2006) Acta Mater 54:157. doi:10.1016/j.actamat.2005.08.036

24. Louzguine DV, Inoue A (2002) J Mater Res 17:1014. doi:10.1557/JMR.2002.0149
25. Kim HS (2000) Mater Sci Eng A 289:30. doi:10.1016/S0921-5093(00)00909-6
26. Kim HS, Hong SI, Kim SJ (2001) J Mater Proc Tech 112:109. doi:10.1016/S0924-0136(01)00565-9
27. Chawla KK (1987) Composite materials, science and engineering, Ch. 10. Springer-Verlag, New York, p 177
28. Kelly A (1971) In: Kelly A, Nicholson RB (eds) Particle and fibre reinforcement in strengthening methods in crystals, Ch. 8. Applied Science Publishers Ltd., London, p 433
29. Bruck HA, Rabin BH (1999) J Mater Sci 34:2241. doi:10.1023/A:1004509220648
30. Mileiko ST (1969) J Mater Sci 4:974. doi:10.1007/BF00555312
31. Kim HS, Warren PJ, Cantor B, Lee HR (1999) Nanostruct Mater 11:241. doi:10.1016/S0965-9773(99)00037-9
32. Sarkar BK, Mukherjee MK, Natarajan A (1982) Z Werkstofftech 13:269
33. Madsen B, Lilholt H (2003) Comp Sci Tech 63:1265. doi:10.1016/S0266-3538(03)00097-6